Extreme Acoustic Metamaterial by Coiling Up Space

Zixian Liang and Jensen Li*

Department of Physics and Materials Science, City University of Hong Kong, Tat Chee Avenue, Kowloon Tong, Kowloon, Hong Kong
(Received 23 August 2011; published 16 March 2012)

We show that by coiling up space using curled perforations, a two-dimensional acoustic metamaterial can be constructed to give a frequency dispersive spectrum of extreme constitutive parameters, including double negativity, a density near zero, and a large refractive index. Such an approach has band foldings at the effective medium regime without using local resonating subwavelength structures, while the principle can be easily generalized to three dimensions. Negative refraction with a double negative prism and tunneling with a density-near-zero metamaterial are numerically demonstrated.

Acoustic metamaterials are engineered materials that exhibit unusual constitutive parameters which are usually constructed from local resonating subwavelength structures [1–9]. Like their optical counterparts, these materials give rise to many novel phenomena including subwavelength focusing [10–16], extraordinary transmission [17–19], and, very recently, invisibility cloaking [20–25]. Alternatively, we can also use phononic crystals to demonstrate similar phenomena. Negative refraction, subwavelength imaging, and gradient index focusing have been demonstrated using this approach [26–28]. Such an approach can avoid local resonance and loss, while pushing the working frequencies to the diffraction regime in which a rigorous effective medium becomes ill defined. Here, we show that by coiling up space, a phononic crystal can be constructed with band foldings at very low frequencies so that it can actually have a valid effective medium description with extreme constitutive parameters. For airborne sound, this would normally require materials such as silicone rubber, which has a very high refractive index but unavoidably high sound attenuation. In our approach, we show that such a high refractive index can be achieved by coiling up space using curled channels of subwavelength cross section. The propagating phase along these curled channels can be arbitrarily delayed in order to mimic a high refractive index. Then, a metamaterial can be constructed from the high index material without any local resonance in order to generate a large dispersive spectrum of constitutive parameters, ranging from negative refractive indices, density near zero to very positive indices. Negative refraction associated with double negativity and tunneling through a density-near-zero metamaterial in two dimensions are also numerically demonstrated. Such a principle of coiling up space can be made isotropic and it can be easily applied to three dimensions.

First, we aim to show how space can be coiled up. In acoustics, waves can propagate within the perforations of subwavelength cross sections in the absence of a cutoff frequency. This concept has been used to generate a large anisotropy [5–9] and subwavelength imaging devices that employ such anisotropy in a fixed direction [12–14]. As an acoustic wave is simply a scalar field, these perforations can be further coiled up, whereas the waves can still propagate freely in the curled space. Figure 1(a) shows a schematic diagram of our metamaterial-repeating units. Identical thin hard solid plates (e.g., brass) of thickness w and length L are inserted into a background fluid (e.g., air) in a way that forms a network of fluid channels of width d. The red dashed lines outline the primitive unit cell of lattice constant a. For example, waves now propagate along a zigzag path, shown in blue arrows, instead of a straight line from point A to C and the space is effectively coiled up by a factor of approximately 4.2 in total path length. The structure is then simplified to that shown in Fig. 1(b) of the same size. The "X"-shaped region now represents the fluid channels that have a higher index n_{0r} (n_{0r} is the relative refractive index normalized to the original background fluid and is approximately the same factor, namely, 4.2), while the rest of the regions represent the hard solid plates. By using such a high refractive index
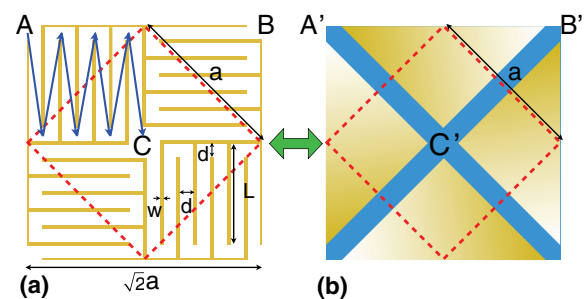
FIG. 1 (color online). (a) Schematic diagram of metamaterial-repeating units in coiling up space. The hard solid plates (thin solid lines) inserted into the background fluid (white color) have a thickness $w = 0.02a$ and a length $L = 0.61a$. The continuous fluid channels have a width $d = 0.081a$, where a is the lattice constant of the primitive unit cell outlined by dashed lines. The connected arrows show the zigzag path of the propagation of acoustic waves, which is equivalent to a high index n_{0r} (relative to the background fluid) in (b) the simplified view with straightened channels ("X"-shaped region).

with materials of negligible loss in constructing the metamaterial, the corresponding band foldings should occur at low frequencies.

A simple model to describe the band structure of the metamaterial can be obtained approximately if we assume the channels in Fig. 1(b) are narrower than a wavelength. By applying the Floquet-Bloch theory, the dispersion relation is expressed as

$$\cos\varphi_{C'A'} + \cos\varphi_{C'B'} = 2\cos(n_{0r}k_0 a), \quad (1)$$

where $\varphi_{C'A'}$ and $\varphi_{C'B'}$, respectively, represent the elapsed phase of a Bloch wave in the $C'A'$ and $C'B'$ directions for the unit cell, k_0 or ω/c is the wave number of the acoustic waves in the background fluid. From Eq. (1), the dispersion relation can be solved. Different branches of the cosine function represent band foldings. Because the metamaterial coils up the space with the same factor n_{0r} in both the $C'A'$ and the $C'B'$ directions, the equifrequency contours (EFCs) should be very close to a circle near the Γ point ($\varphi_{C'A'} = \varphi_{C'B'} = 0$). This generates an isotropic refractive index for the metamaterial. The normalized frequencies $\omega a/(2\pi c)$ for the different branches intersecting at Γ can be found as integral multiples of $1/n_{0r}$. The position of the bands can thus be tuned by n_{0r}, or the path length of the acoustic waves in the coiled space. A longer path length is equivalent to a higher relative refractive index n_{0r}. This results in band foldings in the band structure at low enough frequencies at which an effective medium description with both effective density and bulk modulus is still valid near the Γ point.

Although Eq. (1) describes the qualitative picture of the band structure of the metamaterial, we can numerically obtain the band structure with all the microstructures in a full-wave simulation (COMSOL Multiphysics). The results are shown in Fig. 2(a), where the ΓX direction is defined along CB in Fig. 1(a). Except for the small gaps opening at the Γ and M points (shown by insets a1 to a3) and small frequency shift because of the finite width of the fluid channels, the whole band structure is very well approximated by Eq. (1) (gray dash-dotted lines). At lower frequencies, the channel width is much smaller than the wavelength, and thus the two band structures coincide with each other, e.g., the first band. The slopes around the Γ point in both the ΓX and ΓM directions are almost the same at the first, third, and fifth bands owing to band folding. This indicates isotropic indices and thereby also that the EFCs of the three bands [$\omega a/(2\pi c)$ from 0 to 0.04, from 0.18 to 0.218, and from 0.22 to 0.26] shown in Figs. 2(b) to 2(d) are almost circular with variations in radius within 5%. The different relative indices can then be extracted from the sizes of the EFCs comparing to the sound lines shown by black dashed lines in Fig. 2(a). A large relative index $n_r = 6$ is found for the first band at low frequencies, which is very near to the value 5.9 given by $n_r = \sqrt{2}n_{0r}$ [Eq. (1)]. At the third and fifth bands, negative
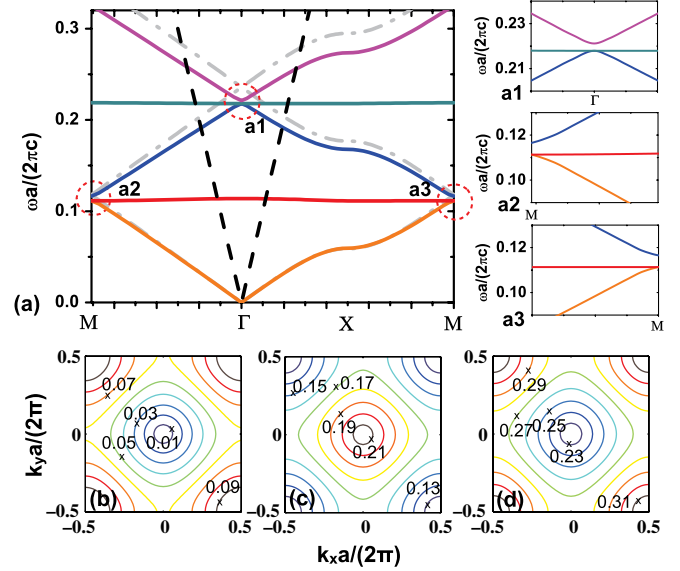
FIG. 2 (color online).   (a) The band structure (solid lines) of the metamaterial. The black dashed lines represent the sound lines of the background fluid. The gray dash-dotted lines show the band structure obtained from Eq. (1) with $n_{0r} = 4.2$. Inset a1 shows the gap opening at the Γ point, and a2 and a3 show the gap opening on both sides of the M point. (b)–(d) The equifrequency contours (EFCs) of the first, the third and the fifth band. $k_{x/y}$ is the Bloch wave number in the CB/CA direction, ω is the angular frequency, and c is the velocity of the waves in the background fluid.

indices from 0 to approximately -1 and positive indices smaller than 1 can be obtained, respectively. We note that there is a flat band around $\omega a/(2\pi c) = 0.219$ at the edge of the band gap in the effective medium region. This band is transverse in nature. For example, by examining the pressure field profiles (results not shown) for the modes along the ΓX or ΓM direction in the simplified view Fig. 1(b), they are actually odd modes regarding the mirror plane containing the k vector. Thus these modes cannot be excited by incident plane waves of longitudinal nature propagating along the same k vector in this picture. However, it is not completely deaf [1] when we go to the microstructure view in Fig. 1(a) because the structure has undergone a mirror-symmetry breaking regarding the incident waves. Here, we only focus on the bands with the longitudinal modes in the effective medium regime.

Indeed, all the above bands of the circular EFCs only span to a normalized frequency 0.26 at which the corresponding wavelength in the background fluid is still at least a few times larger than the lattice constant. The metamaterial can thus be described using an effective medium in more detail. By calculating the complex reflection and transmission coefficients of the unit in Fig. 1(a), we can now resolve the relative effective index n_r and impedance Z_r for the above bands [29]. Owing to the lack of local resonances (those associated with the resonating subwave-

length units in conventional metamaterials) in our approach, the material absorption losses are not amplified and we have neglected these material absorption losses in our model as a simplification. We note that there may still be some material losses in practice. The results are shown in Fig. 3(a) with values of n_r agreeing with the band structure in Fig. 2(a). The effective density and bulk modulus relative to the background fluid are then obtained by $\rho_r = n_r Z_r$ and $B_r = Z_r/n_r$, which are plotted in Fig. 3(b). In this work, all the quantities n_r, Z_r, ρ_r, and B_r are defined normalized to the background fluid. We emphasize that only a refractive index but not both constitutive parameters for a phononic crystal can be defined in the diffraction regime instead of the effective medium regime we are working with here. At the long wavelength limit, ρ_r and B_r are simply constants that also agree with the geometric considerations: $B_r = 1/(1 - f) = 1.23$ where $f = 0.19$ is the filling ratio and relative density $\rho_r = n_r^2 B_r = 44.3$ where $n_r = 6$ is previously found from the zigzag path length. Our approach of coiling up space is effective at achieving a high refractive index which is rare in nature. In the frequency range from 0.18 to 0.26, ρ_r changes from negative to positive and crosses zero at $\omega a/(2\pi c) = 0.218$, which is the lower edge of the band gap, while $1/B_r$ also changes from negative to positive in a similar way and crosses zero at $\omega a/(2\pi c) = 0.22$, which is the upper edge of the band gap. Below the band gap, we thus have a frequency region of simultaneously negative ρ_r and B_r to give $n_r < 0$. Both n_r and Z_r are dispersive in the frequency range. Contrary to the conventional approaches in overlapping two different kinds of resonances to create double negativity, we only need to coil up the space to give a large enough n_{0r}.

Next, we demonstrate two applications using the extreme constitutive parameters given by our approach of coiling up space. First, an acoustic prism that has simultaneously negative density and negative bulk modulus can be constructed using the same structures shown in Fig. 1(a). A corner of the prism is shown in Fig. 4(a) with the inset of a closer view of the microstructures near the edge of the 45° inclination. A Gaussian beam of width $15.4a$ with unit amplitude impinges on the prism from the bottom at a chosen normalized frequency $\omega a/(2\pi c) = 0.191$ in the background fluid. The relative effective index is $n_r = -1$ at the frequency and the beam undergoes negative refraction and exits the prism with amplitude around 0.4 due to impedance mismatch in a horizontal direction in the simulation. Some reflection also occurs at the bottom of the prism (with values outside -1 to 1 due to interference). For comparison, we also simulated the same prism using an effective medium description where the corresponding relative density and bulk modulus ($\rho_r = B_r = -8$) are extracted from Fig. 3(b). The result is shown in Fig. 4(b) with the same Gaussian beam as the input. The output beam direction, amplitude, and phase distribution are well comparable with those in Fig. 4(a), indicating our effective medium that has both negative density and negative bulk modulus faithfully represents the metamaterial.
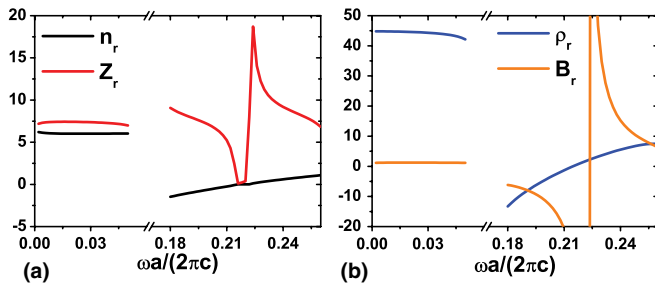
As another example, our structure has a density near to zero at a very low frequency. This is the analog of ε near zero in electromagnetism and can support a novel wave tunneling phenomenon within a waveguide [30]. Figure 5(a) shows the pressure field for such a rectangular waveguide in the acoustic version with a plane wave impinging from the left and a hard solid plate inserted in the middle. Because the solid blocks more than half of the width of the waveguide, the plane wave is scattered severely. In Fig. 5(b), the scatterer is now enclosed by our metamaterial. In both simulations, we chose a normalized frequency $\omega a/(2\pi c) \approx 0.214$ which is a little bit smaller than the frequency of the lower edge of the band gap where the relative effective density is zero. The small relative
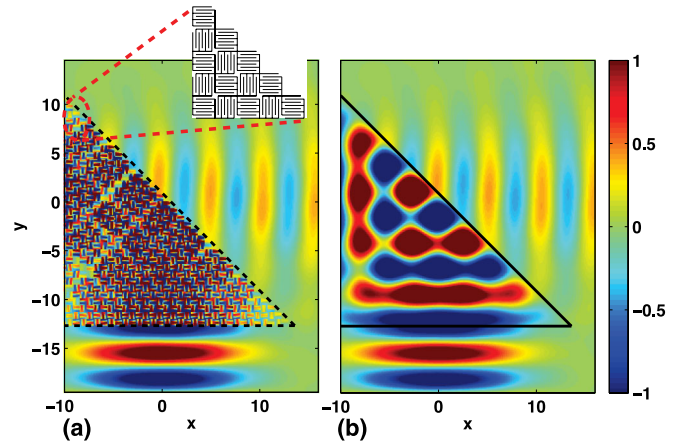
FIG. 4 (color online).   Pressure field pattern with (a) an acoustic prism with microstructures outlined by black dashed lines and (b) the same acoustic prism with the effective medium outlined by black solid lines. The inset of (a) shows a closer view of the prism's microstructure at the edge. The black solid lines represent the hard solid plates. A Gaussian beam of width $15.4a$ impinges on the prism vertically from the bottom at a normalized frequency $\omega a/(2\pi c) = 0.191$ in the background fluid. The corresponding relative effective index is $n_r = -1$. All length scales are normalized to the lattice constant a.

FIG. 3 (color online).   (a) The relative effective index n_r and impedance Z_r vary with normalized frequency $\omega a/(2\pi c)$. (b) The effective mass density ρ_r and bulk modulus B_r vary with $\omega a/(2\pi c)$. All n_r, Z_r, ρ_r, and B_r are parameters normalized to the background fluid.
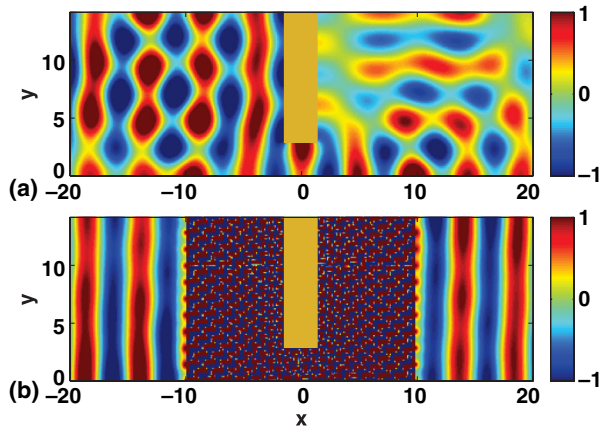
FIG. 5 (color online).   Pressure field pattern of (a) an ideal hard solid plate blocking more than half of the width of a waveguide, and (b) tunneling with the density-near-zero metamaterial at a normalized frequency $\omega a / (2\pi c) \approx 0.214$. A plane wave impinges from the left side in both (a) and (b). The metamaterial has 10×14 units excluding the hard solid region of 8×2 units. All length scales are normalized to the lattice constant a.

effective density $\rho_r = -0.1$ together with the large relative bulk modulus $B_r = -33$ implies the occurrence of tunneling. From Fig. 5(b), the plane wave can now squeeze through the narrow channel and exit the waveguide as a plane wave that has high transmission again.

The presented analysis and numerical results of achieving isotropic extreme constitutive parameters are based on the physical picture of coiling up the space the same ways in both the x and y directions. If we tune the path length in one direction [i.e., CA in Fig. 1(a)] to become longer, anisotropic refractive indices at the first band can be obtained. We can tune the anisotropy by controlling the ratio of the total paths lengths in the two directions. Moreover, if we coiled up the space in the third direction as well, a three-dimensional metamaterial that has extreme indices can be designed similarly. In conclusion, we have proposed a new way of generating a wide dispersive spectrum of acoustic extreme constitutive parameters through coiling up space. By coiling up space, we can obtain high refractive indices in different directions and obtain band foldings at low frequencies at which both the effective density and bulk modulus can be well defined. Such an approach avoids the usage of local resonances to achieve double negativity, density near zero, and very positive refractive indices. We believe our approach in coiling up space will be useful for designing transformation acoustical devices and other acoustic devices requiring extreme constitutive parameters.

*jensen.li@cityu.edu.hk

[1] J. Li and C. T. Chan, Phys. Rev. E **70**, 055602(R) (2004).
[2] N. Fang, D. Xi, J. Xu, M. Ambati, W. Srituravanich, C. Sun, and X. Zhang, Nature Mater. **5**, 452 (2006).
[3] Z. Yang, J. Mei, M. Yang, N. H. Chan, and P. Sheng, Phys. Rev. Lett. **101**, 204301 (2008).
[4] S. H. Lee, C. M. Park, Y. M. Seo, Z. G. Wang, and C. K. Kim, Phys. Rev. Lett. **104**, 054301 (2010).
[5] D. Torrent and J. Sanchez-Dehesa, Phys. Rev. Lett. **105**, 174301 (2010).
[6] A. N. Norris and A. J. Nagy, J. Acoust. Soc. Am. **128**, 1606 (2010).
[7] J. B. Pendry and J. Li, New J. Phys. **10**, 115032 (2008).
[8] I. Spiousas, D. Torrent, and J. Sanchez-Dehesab, Appl. Phys. Lett. **98**, 244102 (2011).
[9] A. V. Amirkhizi, A. Tehranian, and S. Nemat-Nasser, Wave Motion **47**, 519 (2010).
[10] X. Zhang and Z. Liu, Appl. Phys. Lett. **85**, 341 (2004).
[11] S. Zhang, L. Yin, and N. Fang, Phys. Rev. Lett. **102**, 194301 (2009).
[12] J. Li, L. Fok, X. Yin, G. Bartal, and X. Zhang, Nature Mater. **8**, 931 (2009).
[13] H. Jia, M. Ke, R. Hao, Y. Ye, F. Liu, and Z. Liu, Appl. Phys. Lett. **97**, 173507 (2010).
[14] J. Zhu, J. Christensen, J. Jung, L. Martin-Moreno, X. Yin, L. Fok, X. Zhang, and F. J. Garcia-Vidal, Nature Phys. **7**, 52 (2011).
[15] H. J. Lee, H. W. Kim, and Y. Y. Kim, Appl. Phys. Lett. **98**, 241912 (2011).
[16] X. Zhou and G. Hu, Appl. Phys. Lett. **98**, 263510 (2011).
[17] M. H. Lu, X. K. Liu, L. Feng, J. Li, C. P. Huang, Y. F. Chen, Y. Y. Zhu, S. N. Zhu, and N. B. Ming, Phys. Rev. Lett. **99**, 174301 (2007).
[18] J. Christensen, L. Martin-Moreno, and F. J. Garcia-Vidal, Phys. Rev. Lett. **101**, 014301 (2008).
[19] H. Estrada, P. Candelas, A. Uris, F. Belmar, F. J. G. de Abajo, and F. Meseguer, Phys. Rev. Lett. **101**, 084302 (2008).
[20] S. A. Cummer and D. Schurig, New J. Phys. **9**, 45 (2007).
[21] H. Chen and C. T. Chan, Appl. Phys. Lett. **91**, 183518 (2007).
[22] M. Farhat, S. Enoch, S. Guenneau, and A. B. Movchan, Phys. Rev. Lett. **101**, 134501 (2008).
[23] A. N. Norris, J. Acoust. Soc. Am. **125**, 839 (2009).
[24] S. Zhang, C. Xia, and N. Fang, Phys. Rev. Lett. **106**, 024301 (2011).
[25] B.-I. Popa, L. Zigoneanu, and S. A. Cummer, Phys. Rev. Lett. **106**, 253901 (2011).
[26] M. H. Lu, C. Zhang, L. Feng, J. Zhao, Y. F. Chen, Y. W. Mao, J. Zi, Y. Y. Zhu, S. N. Zhu, and N. B. Ming, Nature Mater. **6**, 744 (2007).
[27] A. Sukhovich, B. Merheb, K. Muralidharan, J. O. Vasseur, Y. Pennec, P. A. Deymier, and J. H. Page, Phys. Rev. Lett. **102**, 154301 (2009).
[28] T. P. Martin, M. Nicholas, G. J. Orris, L. W. Cai, D. Torrent, and J. Sanchez-Dehesa, Appl. Phys. Lett. **97**, 113503 (2010).
[29] D. R. Smith, D. C. Vier, Th. Koschny, and C. M. Soukoulis, Phys. Rev. E **71**, 036617 (2005).
[30] M. Silveirinha and N. Engheta, Phys. Rev. Lett. **97**, 157403 (2006).